Radar Measurement of Rainfall with and without Polarimetry

CARLTON W. ULBRICH

Department of Physics and Astronomy, Clemson University, Clemson, South Carolina

DAVID ATLAS

Laboratory for Atmospheres, NASA Goddard Space Flight Center, Greenbelt, Maryland

(Manuscript received 12 June 2007, in final form 26 November 2007)

ABSTRACT

Raindrop size distributions (DSDs) for tropical convective storms are used to examine the relationships between the parameters of a gamma DSD, with special emphasis on their variation with the stage of the storm. Such a distinction has rarely been made before. Several storms from a variety of tropical locations are divided into storm stages according to the temporal dependence of their reflectivity factor Z, rainfall rate R, and median volume diameter D_0. In most cases it is found that the DSD parameter D_0 is approximately constant in time during the convective, or C, stage, which leads to a Z–R relation of the form $Z = AR$, that is, a linear relationship between Z and R. This finding implies the existence of equilibrium DSDs during the C stage. The convective stage is sometimes marked by pulsations in draft strength so that D_0, R, and Z and associated values of the shape parameter μ decrease in a quasi-transition stage before increasing once more. Theoretical relations between the differential reflectivity Z_{DR} and the ratio Z/R as functions of the DSD parameter μ are derived by assuming a gamma DSD and an accurate raindrop fall speed law. It is found that data derived from disdrometer observations lie along a $\mu = 5$ isopleth for tropical continental C stages (Puerto Rico and Brazil) and along a $\mu = 12$ isopleth for tropical maritime C stages [Tropical Ocean and Global Atmosphere Coupled Ocean–Atmosphere Response Experiment (TOGA COARE)]. Small values of μ that occur in the weak updraft intervals do not impact the rainfall measurements because they correspond to relatively small R. The latter features imply that the measurement of rainfall for the convective stages can be performed with standard polarimetry involving only two measurables rather than three, provided knowledge of μ is available a priori. A new rain parameter diagram is presented in which isopleths of the generalized number concentration and D_0 are superimposed on the Z–R plot. It is proposed that it is possible to estimate D_0 from climatological and observable storm structural features, which, with Z, provide estimates of R. Such an approach is necessary for use with conventional radars until polarimetric radars are more widely available.

1. Introduction

In two prior papers (Atlas and Ulbrich 2006; Ulbrich and Atlas 2007, hereinafter UA07) the gamma parameter diagram was introduced as a means of characterizing the drop size distribution (DSD) in convective storms. Such storms typically comprise convective (C), transition (T), and stratiform (S) stages. Stage C commonly features nearly uniform or equilibrium DSD with narrow width with near-constant median volume diameter D_0. The essence of such a DSD is that it defines a family of equilibrium curves defined by $f_N(D, R) = Rf_N(D)$, where R is rain rate and $f(D)$ is the shape function for number concentration (List 1988). This means that all of the moments of $f_N(D)$ are constant and independent of R and N_T (N_T is the total number of drops per unit volume). One of the main consequences is that the radar reflectivity factor Z, which is proportional to the sixth moment, is linearly related to R. That is, $Z = AR^b$, where $b = 1$. So too are other integral parameters linearly related to one another. (In this work the term reflectivity factor Z refers to the reflectivity factor at horizontal polarization: Z_H.)

We acknowledge List (1988, and subsequent collaborative work) and his colleagues for their seminal work on equilibrium DSDs and Hu and Srivastava (1995) for

Corresponding author address: C. W. Ulbrich, 106 Highland Dr., Clemson, SC 29631.
E-mail: cwu@nctv.com

DOI: 10.1175/2007JAMC1804.1

© 2008 American Meteorological Society

an exceptionally insightful theoretical analysis of the processes involved. A recent study by Uijlenhoet et al. (2003) also provides strong evidence for the existence of equilibrium DSDs. The reader is referred to a number of other works on the subject in the latter two papers.

Despite this basic work on equilibrium DSDs, it is curious that the large collection of Z–R relations in the literature (Battan 1973; Rosenfeld and Ulbrich 2003) shows only a rare value of the exponent $b = 1$ in the $Z = AR^b$ relation characteristic of such DSDs. Only Fujiwara (1965) shows a few cases of $b \approx 1$ in convective storms. This is due to the failure of most investigators to divide convective rains into their C, T, and S stages and the occurrence of intervals of small D_0 (median volume or mass diameter) between successive peak updrafts.

Using data gathered during the Tropical Ocean and Global Atmosphere Coupled Ocean–Atmosphere Response Experiment (TOGA COARE), Tokay et al. (1999) did classify the stages into C and S. However, they included the transition stage within C, or within a "mixed convective–stratiform" class, thus failing to find equilibrium DSDs. Their average values of Z, and D_0, and μ (the shape parameter in the gamma DSD) are also considerably smaller than those found by UA07 for some of the same storms. Atlas et al. (1999) subsequently used the C, T, and S classification in the same experiment and found three days on which $b \approx 1$ during the C stages. They also showed that the coefficient A is proportional to $D_0^{2.33}$. Well-formed equilibrium DSDs were found on 17 January 1993 (Atlas and Ulbrich 2000). The present paper has two primary thrusts. The first is to demonstrate that the rain rate can be determined accurately from measurements of Z and Z_{DR} not only for equilibrium DSDs but also for any DSD. In particular, it will be demonstrated that there is a distinct difference between the R/Z–Z_{DR} relations for stage-C rains in tropical continental and maritime storms according to the breadth of the DSD and/or number concentration. The second thrust is to show that, because of the latter DSD differences in convective storms and their sharp contrast with those of stratiform storms (Bringi et al. 2003, hereinafter BAL03; UA07), it is possible to estimate rainfall from the climatological values of number concentration and Z alone, thus providing a capability to use a conventional radar without polarimetric capability until the latter is more broadly available.

This work pertains directly to S-band (10 cm) radar but can be translated to C-band (6 cm) radar. For example, Bringi and Chandrasekar (2001, hereinafter BC) present Z_{DR}–Z relations for C band. Also, we do not consider the possible effects of anomalous propagation, although we do not believe that they are of concern in the well-mixed atmosphere accompanying convective storms. An exception may be due to the cooling of the lower levels by evaporation—a process that affects targets behind the storm such as reported by Battan (1973, 26–28).

2. Background

In what follows, the DSD will be assumed to have the form of the gamma function given by

$$N(D) = N_0 D^{\mu} \exp(-\Lambda D), \tag{1}$$

where D is drop diameter, μ is the shape parameter (inversely related to the normalized breadth of the DSD), and Λ is the slope of the tail. Also,

$$\Lambda D_0 = 3.67 + \mu \quad \text{and} \tag{2}$$

$$N_W = \frac{4^4}{\pi \rho_w}\left(\frac{W}{D_m^4}\right). \tag{3}$$

Here N_W is the generalized number concentration of an exponential DSD having the same liquid water content W and mass-weighted diameter D_m as the actual DSD (Testud et al. 2001).

This work uses the theoretical relation between the differential reflectivity Z_{DR} and the median volume diameter D_0 derived by BC expressed in the form

$$Z_{DR} = 0.295 D_0^{2.058}. \tag{4}$$

The Z_{DR} values were found using theoretical values of the backscattering cross sections at horizontal and vertical (H and V) polarizations. The experimental D_0 values were computed directly from the DSDs and not from values of Z_{DR} using the empirical relation in Eq. (4). Empirical Z_{DR}–D_0 fits have been performed for each storm. The results (not shown) demonstrate that Eq. (4) is very well satisfied for all four stages of the Arecibo, Puerto Rico, storm over the full range of observed D_0. Thus the scale on the right side of Fig. 3 (described below) must, by definition, agree with the experimental values of D_0 found from the DSDs in this work. A dependence on the parameter μ is implicit, as shown in Fig. 1 where Z_{DR} is plotted versus D_0 with μ as a parameter. Equation (4) is shown as dashed in Fig. 1. It is seen that, as D_0 increases, Eq. (4) crosses lines of constant μ toward smaller values. In the range $1 < D_0 < 2$ mm, Z_{DR} initially follows the curve for $\mu = 4$; for $2.0 < D_0 < 3.0$, Z_{DR} lies between curves for $\mu = 3$ and $\mu \approx 1$. Although these ranges of μ may not seem appreciable, the changes in Z_{DR} are large.

It will be shown in section 3 that the dependence of R, Z, and Z_{DR} on both D_0 and μ produces a plot of Z_{DR} versus R/Z that involves isopleths of μ. Nevertheless it

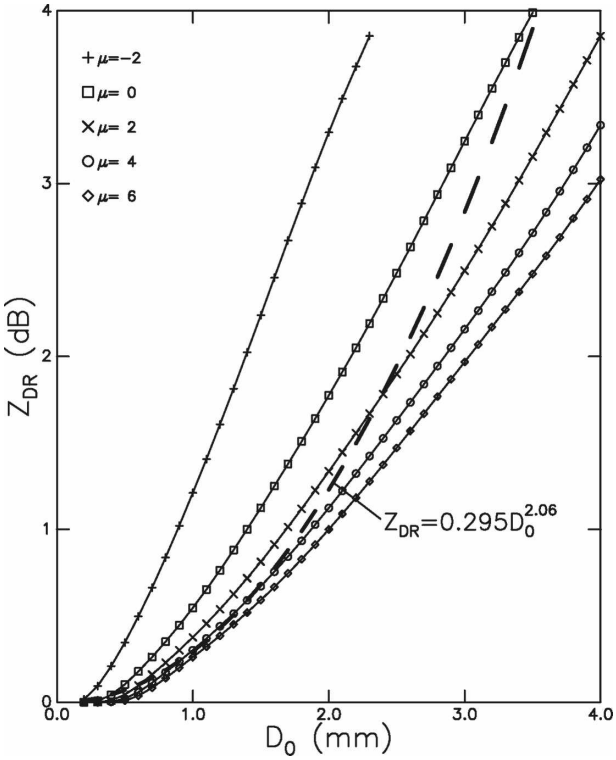

FIG. 1. The Z_{DR} vs D_0 with μ as parameter. The dashed curve is from Bringi and Chandrasekar (2001).

will be seen that, for certain classes of storms, data for Z_{DR} and R/Z (from disdrometer measurements) lie predominantly along two preferred isopleths: $\mu = 5$ for continental tropic storms and $\mu = 12$ for maritime tropical storms. This implies that knowledge of μ (from climatological data, say) permits accurate measurement of R from only two measurables: Z_{DR} and Z. It is not surprising that such empirical Z_{DR}–R/Z relations depend on μ in different ways from the Z_{DR}–D_0 plots. This follows from the fact that there are three integral parameters involved in the Z_{DR}–R/Z plots, each of which weighs their integrands differently with respect to μ. Thus, the use of the Z_{DR}–D_0 relation to determine D_0 automatically accounts for the variation with μ, but a constant value of μ suffices in the determination of R from the Z_{DR}–R/Z relation.

3. Observations

The time history of Z, R, D_0, and N_W based upon 2-min samples with the Joss–Waldvogel (J–W) disdrometer made at Arecibo on 15 October 1998 (previously shown in UA07, their Fig. 2) is presented here with the addition of a record of 2-min samples of μ. This storm was classified as continental. It comprised two major convective cells followed by transition and stratiform stages.

TABLE 1. The Z–R analyses for the Arecibo storm on 15 Oct 1998 considered in this work. Labels C, T, and S denote the period of rainfall as convective, transition, or stratiform, respectively. Parameters A and b are the coefficient and exponent in an empirical relation of the form $Z = AR^b$, N is the total number of drop size spectra used in the fits, and H is the total depth of rainfall during each period.

Period	Times (LT)	A	b	N	H (mm)	% of total
C1	1435–1455	2754	0.90	21	28.48	60.40
C2	1456–1534	1471	0.96	39	16.83	35.70
C1 + C2	1435–1534	906	1.13	60	45.31	96.1
T	1535–1608	310	1.46	34	1.36	2.88
S	1609–1705	280	1.46	54	0.48	1.02
All	1435–1705	294	1.44	148	47.15	100.0

Table 1 presents key statistics corresponding to Fig. 2. Note that stages C1 and C2 with the largest Z and D_0 values are responsible for a total accumulation of 45.3 mm, or 96% of the total rain, although they occur only 45% of the time. Because of the high 0°C level and the absence of a bright band, the generation mechanism has been identified as a mix of warm and cold processes. Stage C1 is characterized by equilibrium DSDs of large D_0 and maximum Z. Stage C2 has slightly smaller and more variable Z and D_0, but the DSDs are also close to equilibrium. This stage differs sharply from C1; that is, it is marked by several subcells, each with a maximum and trailing minimum. Such peaks and troughs are attributable to the coupling of the updrafts and water content that is caused by successive precipitation loading and unloading (Srivastava 1967, and references therein; Battan 1973, p. 26).

A better picture of the events requires the examination of the fluctuations in D_0, Z, R, and N_W. Because Z and R are approximately proportional to the 7th and 4.67th power of D_0 and are directly proportional to N_W, we must understand how these variables interact. Note that the first sharp minimum in the D_0, Z, R triplet in stage C2 occurs just after the end of period C1 where the small drops trail off from the neighboring large convective cell as generally expected and as observed on the PPI (UA07, their Fig. 4).

The first sharp peak in stage C2 with $D_0 = 2.8$ mm at 1504 LT is accompanied by a sharp minimum in N_W in accord with Eq. (4). The nearly 10-fold decrease in N_W thus produces minima in Z and R at 1506 LT. It is the broad maximum in D_0 between 1503 and 1508 LT that is associated with the high-reflectivity cell seen in the RHI in Fig. 4a of UA07. The next maximum in Z and R at 1514–1517 LT is associated mainly with the increase of N_W and a small increase in D_0. Also, the trailing decrease in Z and R from 1522 to 1534 LT is marked by a significant decrease in N_W while D_0 re-

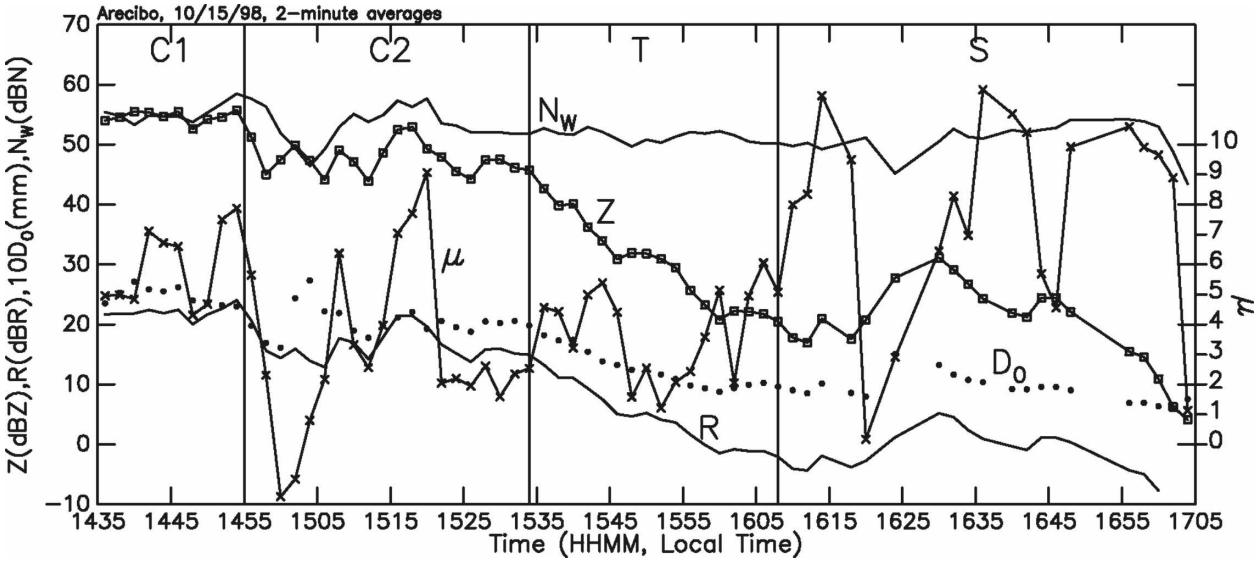

FIG. 2. Time dependence of R (dBR), Z (dBZ), D_0 (mm), μ, and N_W (dBN) at Arecibo on 15 Oct 1998.

mains steady at ~2.0 mm. Note that the deep decrease $\mu < 2$ in the 10-min period at the start of stage C2 is due to the brief transition period at the end of stage C1. The 13-min period at the end of stage C2 is associated with a shelf of intermediate reflectivity (about 40 dBZ) on the RHI. It is evident from this exercise that it is not easy to identify sharp bounds to the various stages. Because the Weather Surveillance Radar—1988 Doppler (WSR-88D) observations referred to here were on a 6-min volume scan repeat cycle, we were unable to associate the smaller-scale Z fluctuations with corresponding features in the radar structure.

We remind the reader that the exponent b in the $Z = AR^b$ relation is given by $b = \Delta(\mathrm{dB}Z)/\Delta(\mathrm{dB}R) = 1 + 23.8[\langle\Delta(\log D_0)\rangle/\langle\Delta(\mathrm{dB}R)\rangle]$ (Atlas et al. 1999).[1] Thus, in any region or period during which the average D_0 is nearly constant, $b \approx 1$. This is the source of $b = 0.96$ for stage C2 in Table 1. In short, the DSDs in C2 are approximately in equilibrium despite the short-term fluctuations in the parameters.

The reader will also note the very sharp fluctuations in μ during the stratiform (S) period, some of which correspond to very narrow DSDs with $\mu \approx 9$–13 and broad ones with $\mu < 0$. We have computed 5-min-average DSDs for the entire S period (not shown). They are based on very small numbers of drops so that their characteristics are unreliable. The very narrow (large μ) DSDs are due to a lack of both large and small drops. The deficit of small drops is almost surely due to the fact that the small ones approach the threshold size of 0.35 mm of the J–W disdrometer. On the other hand, the small-μ, near-exponential DSDs are based upon so few drops as to be artifacts.

4. Relation of R/Z to Z_{DR}

The appendix presents the derivation of the ratio R/Z as a function of Z_{DR}. A similar form was derived by BC. The difference is that they used a relation between fall velocity $v(D)$ and drop diameter D of the form $v(D) = 16.7D^{0.67}$ rather than the more accurate fall speed relation of Atlas et al. (1973).

Figures 3a,b illustrate the relationship of Z_{DR} (left ordinate) and D_0 (right ordinate) to R/Z with μ as a parameter. At constant Z_{DR} the ratio of R/Z varies by only 2.5 dB for $0 < \mu < 12$. We have also superimposed the observations from UA07 of D_0 and R/Z in the C stages of the convective storms in maritime (Fig. 3b; TOGA COARE) and continental {Fig. 3a; Arecibo and Brazil [Large-Scale Biosphere–Atmosphere Experiment in Amazonia (LBA)]} regimes.

Power-law regression relations have been fitted to the data with the results

$$Z_{DR} = 1.23 \times 10^{-3}(R/Z)^{-0.791} \text{ (maritime; } \mu = 12) \quad \text{and} \tag{4a}$$

$$Z_{\mathrm{DR}} = 4.08 \times 10^{-3}(R/Z)^{-0.811} \text{ (continental; } \mu = 5). \tag{4b}$$

[1] The exponent 23.8 in the latter relation differs negligibly from the form that uses the power-law fall speed approximation; it has been verified by a regression of values of A versus D_0 [from Eq. (5) below] for integer values of $0 < \mu < 15$ (not shown).

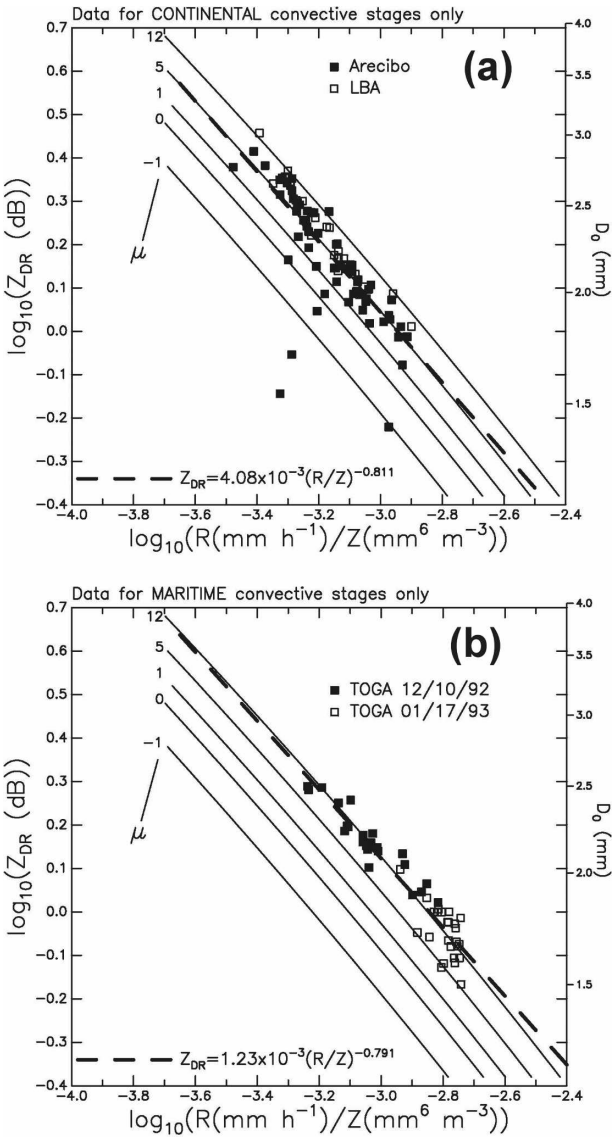

FIG. 3. (a) $\mathrm{Log}_{10}[Z_{\mathrm{DR}}(\mathrm{dB})]$ vs $\log_{10}(R/Z)$ for continental convective stages C for the Arecibo and LBA storms. The isopleths are labeled with their corresponding values of μ. (b) As in (a), but for C stages of two convective storms during TOGA COARE.

The average values $\langle\mu\rangle = 12$ and 5, respectively, are consistent with the finding that tropical continental C rains produce larger drops (D_0) in smaller concentrations than do maritime C rains (BAL03; Fig. 9 of UA07). Although we see that there are a number of points of $\mu < 5$, we have shown in section 3 that almost all of these correspond to small rain rates that contribute little to the total. Such small values of μ are in accord with the existence of near-exponential DSDs expected at the end of each convective thrust.

In addition, note that maritime C stages are characterized by both weaker updrafts and smaller D_0 than the continental C stages. Moreover, for the same liquid water content W, the distribution of water is concentrated near the larger D_0 in maritime storms, that is, in narrower DSDs with smaller normalized distribution of water mass $[(\sigma_m)/D_m]$ and larger μ (BAL03, their Fig. 5).

It is reasonable to suggest that the finding that continental convective storms are characterized by a small number of large drops, and the converse in maritime storms, is due to the larger number of cloud condensation nuclei (CCN) over the continents than over the oceans; these in turn influence the size distribution of cloud droplet sizes (Pruppacher and Klett 1978, p. 227). The larger number of CCN results in a correspondingly large number of small cloud droplets (Pruppacher and Klett 1978, their Fig. 2-6). Rosenfeld (2000) has used multiwavelength satellite measurements to deduce the particle size distributions in clouds; he found that the polluted regions downstream of power plants failed to contain significant number of cloud droplets larger than the critical drop diameter of 25 μm, the size that defines the threshold for the onset of precipitation. This has led to further work demonstrating the decrease in precipitation resulting from air pollution and smoke from fires (Rosenfeld et al. 2007; Andreae et al. 2004). In accord, the paucity of large cloud droplets leads to a corresponding paucity of initial large raindrops that can grow even larger by collection of the cloud water in the smaller size portion of the cloud droplet spectrum. We believe that this is essentially the mechanism responsible for the distinct differences found by BAL03 and UA07 in continental and maritime regions.

The implication of the finding that R/Z is dependent only upon D_0 for distinct values of μ confirms what was known from the start: that is, there is a linear $Z = AR$ relation for each D_0 and corresponding Z_{DR}. This has also been shown more recently by BC [their Eqs. (7.69) and Fig. 7.19]. We may tentatively use $\mu = 5$ or 12 for continental or maritime C stage rain, respectively. However, because of the variability in D_0 and N_W from storm to storm (BAL03) further study is required to determine whether it is necessary to consider such variability. Figure 4 shows a plot of the coefficient A versus D_0 with μ as a parameter.

Using ground-based drop size observations made by Mueller (1962) with the Illinois State Water Survey raindrop camera in Miami, Florida, Uijlenhoet et al. (2003) showed that the exponent b approached 1 and the coefficient A increased to values of about 1700 as the average rain rate approached 100 mm h^{-1} (their Fig. 5). This is consistent with Fig. 4 for values of $1.5 < D_0 < 3$ mm, depending on μ. They conclude that such behavior "indicates a change from a combination of

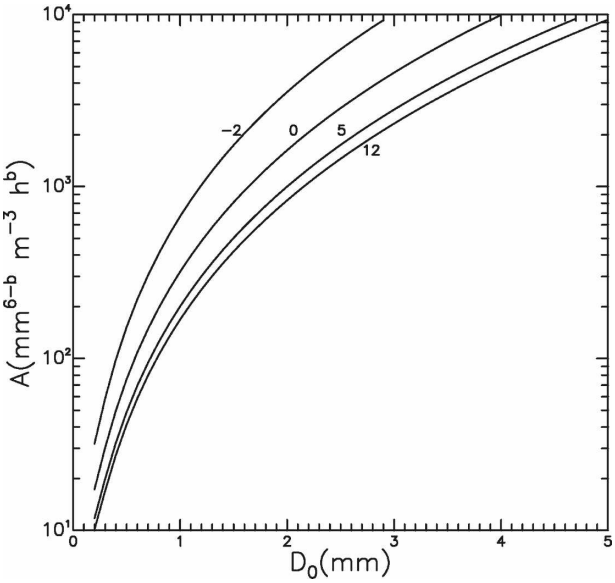

FIG. 4. Variation of the coefficient A in the relation $Z = AR$ for equilibrium DSDs as a function of D_0 for values of $\mu = -2$, 0, 5, and 12. The isopleths are labeled with their corresponding values of μ, increasing from left to right.

size- and number-controlled variability to a situation where the rainfall variability is almost purely number controlled, consistent with equilibrium conditions." The increase of A with rain rate is due to the enhanced rate of collision and coalescence (Hu and Srivastava 1995).

5. Testing the $R = Z/A$ relation

To test the utility of the $R = Z/A$ relation, Fig. 4 has been used to select the values of A corresponding to the 1-min values of D_0 and μ calculated for each DSD and for each stage of the Arecibo storm. This value of A is then used to calculate R_{CALC} minute by minute. The results are compared with the actual values of R_{DISD} found from the disdrometer data in Figs. 5a–d for stages C1, C2, T, and S, respectively. The quantities Δ, δ, and σ shown in each figure correspond to the average deviation (%), the absolute average deviation (%), and the standard deviation (mm h^{-1}) of R_{CALC} from R_{DISD}, respectively; δ is less than 17% in all four stages, which must be considered very good when compared with methods that use empirical Z–R relations. The limitation of this method, however, is that the values of D_0 and μ must be known for each sample. To circumvent this difficulty, a second simulation has been performed in which it is assumed that the values of D_0 and μ are constant during each stage. For the purpose of this simulation, it will be assumed that D_0 is equal to the average value found from the disdrometer data in each stage and that, in accordance with the empirical fits shown in Fig. 3, μ will be assumed to be equal to 5. It follows from Eq. (A1) in the appendix that $Z = AR$, where

$$A = \frac{10^6\Gamma(7+\mu)D_0^3}{0.6\pi\Gamma(4+\mu)(3.67+\mu)^3} \times \left[9.65 - 10.3\left(1 + \frac{6D_0}{3.67+\mu}\right)^{-(4+\mu)}\right]^{-1}. \quad (5)$$

By substituting the values of $\mu = 5$ and $D_0 = (D_0)_{\mathrm{AVE}}$ for each stage of the storm, A is found from Eq. (5) and then R_{CALC} is found from $Z = AR$ for each minute and is compared with R_{DISD}. The results are shown in Fig. 6, in which it is seen that the results for the C1 and C2 stages are in very good agreement with the R_{DISD} values. This is not surprising because the experimental D_0 values for these stages are effectively constant with time. However, during the T stage when D_0 decreases systematically with time (Fig. 2), R_{CALC} overestimates the rain at the beginning and underestimates it toward the end of the stage. It is only near the middle of this period during which time $D_0 = (D_0)_{\mathrm{AVE}}$ that the correct average R is measured properly. When one is concerned with excessive variability during any one stage, we suggest dividing that period into smaller segments of ΔD_0 to enhance accuracy. Of course, the total rain during any period will be accurate if one simply measures $\langle R \rangle$ and the time T for that average.

6. Conventional radar

Until now it has been assumed that it is necessary to use either a polarimetric radar to measure Z_{DR} and D_0 or another dual-parameter method such as the dual-wavelength method of Meneghini and Liao (2007). We now explore the idea of deducing D_0 from the physical and climatological conditions and the associated geometric features of the echo patterns.

This work and its predecessors have emphasized the importance of D_0 and N_W or μ in the measurement of rainfall. We now have abundant evidence of the physical and climatological factors that control the nature of the DSD and the value of D_0. This subject has been covered in considerable depth by Rosenfeld and Ulbrich (2003). They have shown the essential features of DSDs resulting from coalescence, breakup, and evaporation. They have also ordered the variations in liquid water content and D_0 as a function of continental, intermediate, maritime, and orographic classes in general agreement with the findings of BAL03 and UA07. These factors and the structural features of clouds and

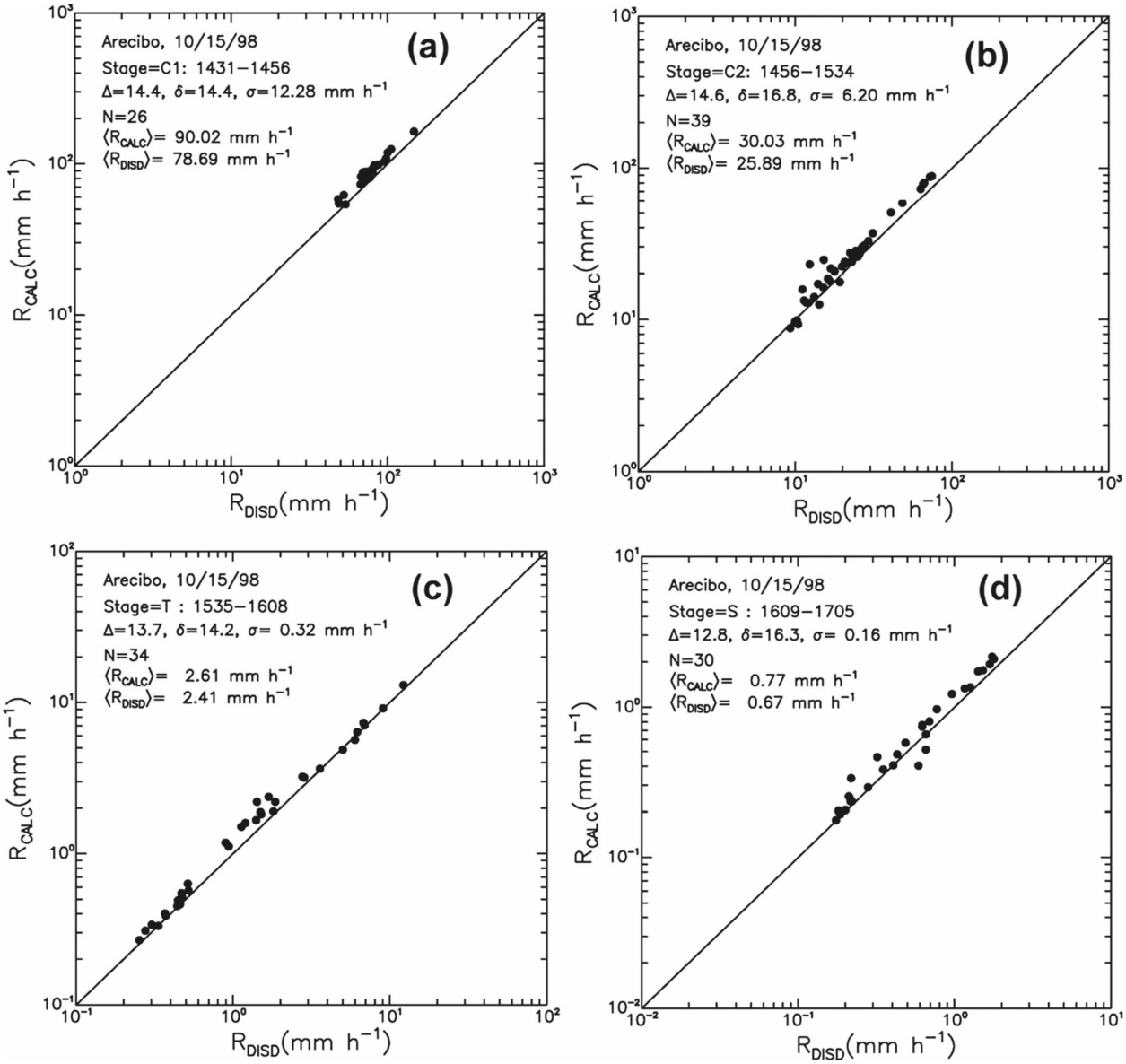

FIG. 5. Comparison of the calculated rainfall rates R_{CALC} with the disdrometer rainfall rates R_{DISD} for the four stages of the storm at Arecibo on 15 Oct 1998: (a) C1, (b) C2, (c) T, and (d) S. Values of R_{CALC} were found using the method in which the values of D_0 and μ for each DSD are used to compute A from Fig. 4 and then $R_{\mathrm{CALC}} = Z/A$. Here, Δ (%), δ (%), and σ (mm h^{-1}) are the average deviation, absolute average deviation, and root-mean-square deviation of R_{CALC} from R_{DISD}, respectively.

storms seen visually from space or radar provide a means of identifying D_0 and N_W in real time. For example, convective cells and stratiform rain can be discerned with ease. It has been shown that the mean and mode of the probability distribution of R increase with the height of the storm (Rosenfeld et al. 1990) and that Z and R determine D_0, conditional on the continental or maritime nature of the storm. Indeed, it has recently been shown that D_0 increases with the radar tops of the cells in typhoons (Chang and Chen Wang 2007). Estimates of updraft speed can be made from the rate of growth of storm tops or from a combination of Doppler velocity measurements and conventional radio soundings. In addition, the occurrence of lightning assures us that the precipitation starts in the ice phase above the 0°C level; its frequency of occurrence is a rough proxy for the updraft strength. Drop number concentrations alone can be approximated both climatologically and physically in the sense that a region of very large Z, near the asymptotic value of 50 dBZ, implies very large

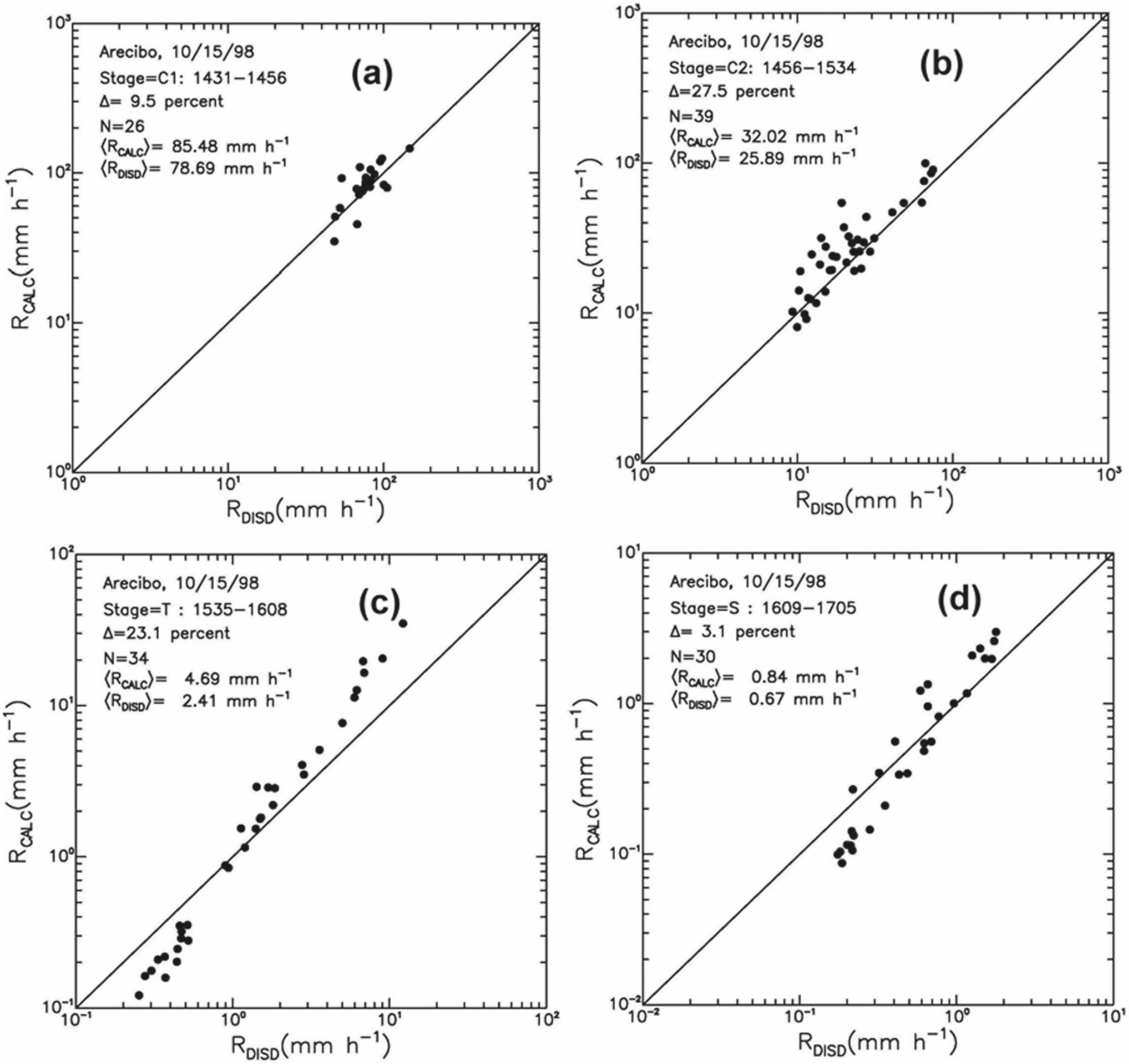

FIG. 6. As in Fig. 5, but for the method in which R_{CALC} is found by assuming D_0 is constant and equal to the average value for each stage. In addition, it is also assumed that $\mu = 5$; Δ, δ, and σ are as in Fig. 5.

D_0 near its asymptote of 3.0 mm (UA07, their Fig. 7). All these characteristics set the boundary conditions for the use of models to predict D_0. In short, we suggest that the stage is set to make reasonable estimates of D_0 without polarimetric radar and thus to estimate rainfall with conventional weather radars. This is a challenge to both cloud physicists and radar meteorologists.

These concepts are illustrated in Fig. 7 showing a new Z–R rain parameter diagram with isopleths of D_0 and N_W. Of course, Z_{DR} is a proxy for D_0. This graph applies strictly to a value of $\mu = 5$; changes in μ cause only small changes in Z and R (appendix). Superimposed in Fig. 7 are the regions of maritime and continental convective and stratiform rains as reported by BAL03 and UA07. Transient zones of small N_W and large D_0 such as occur at the start of an intense convective rain occupy the region of about $25 < Z < 40$ dBZ and $R < 10$ mm h^{-1}. Unusually large concentrations of small drops will be found below the stratiform area. An excellent summary of the various microphysical properties of stratiform rain may be found in BAL03 (related to the discussion of their Fig. 10). The reader may readily experiment with this diagram in Fig. 7 to find the properties of any DSD from Z–R relations or the converse.

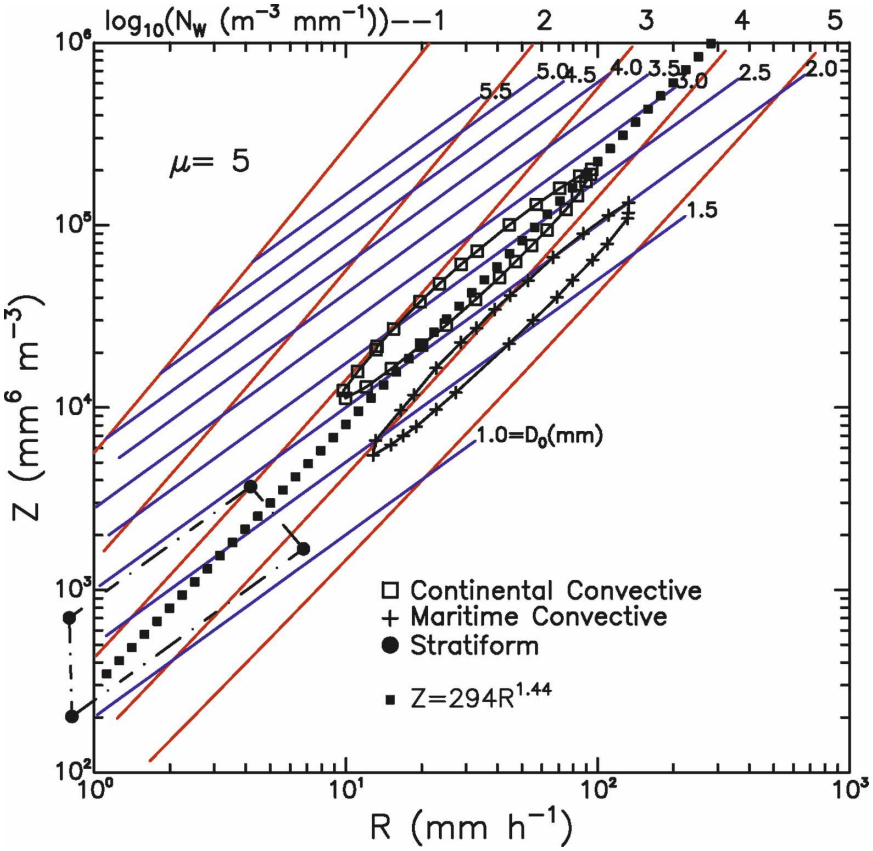

FIG. 7. Advanced rain parameter diagram of Z vs R with isopleths of median volume diameter D_0 (solid blue lines) and generalized number concentration N_W (solid red lines) for a value of $\mu = 5$. Areas of stratiform (dashed), convective maritime (plus signs), and continental (open squares) rains are outlined. The filled squares depict the overall $Z = 294R^{1.44}$ relation for Arecibo, which includes all four stages, C1, C2, T, and S. Note that N_W increases and D_0 decreases diagonally downward to the right.

The overall relation for Arecibo, $Z = 294R^{1.44}$, has been superimposed in Fig. 7. It is almost identical to the default relation of $300R^{1.40}$ for the WSR-88D. Thus, the default relation gives a first-guess approximation to R, D_0, and N_W from a measurement of Z alone.

7. Conclusions

The six-decade rarity of radar reflectivity–rainfall (Z–R) relations characteristic of equilibrium DSDs is due largely to the failure to subdivide convective rains into convective, transition, and stratiform stages. An additional factor is the natural fluctuations in the DSDs resulting from pulsations in the smaller-scale updrafts often found embedded in the larger-scale convective cells. Both disdrometer and polarization measurements have suffered from this deficiency. When it is properly classified, one finds that the convective stage commonly features essentially constant median volume diameter D_0. The result is a linear relation $Z = AR$ in which A is proportional to $D_0^{2.38}$ and virtually insensitive to μ. This permits the definition of A as a function of Z_{DR} or D_0, or its average for all stages (C, T, and S). Two test cases demonstrate the method.

Furthermore, the finding that maritime and continental convective storms occupy different domains in D_0 and number concentration space and do not overlap the stratiform domain suggests that it is possible to estimate number concentration and D_0 from physical and climatological considerations and, along with Z, to estimate rain rate. Such an approach is necessary for use with conventional radars until polarimetric systems become broadly available.

Acknowledgments. We are grateful for the continued hospitality of our parent institutions. We also appreciate the perceptive comments of the anonymous reviewers that have led to the improvements in this paper.

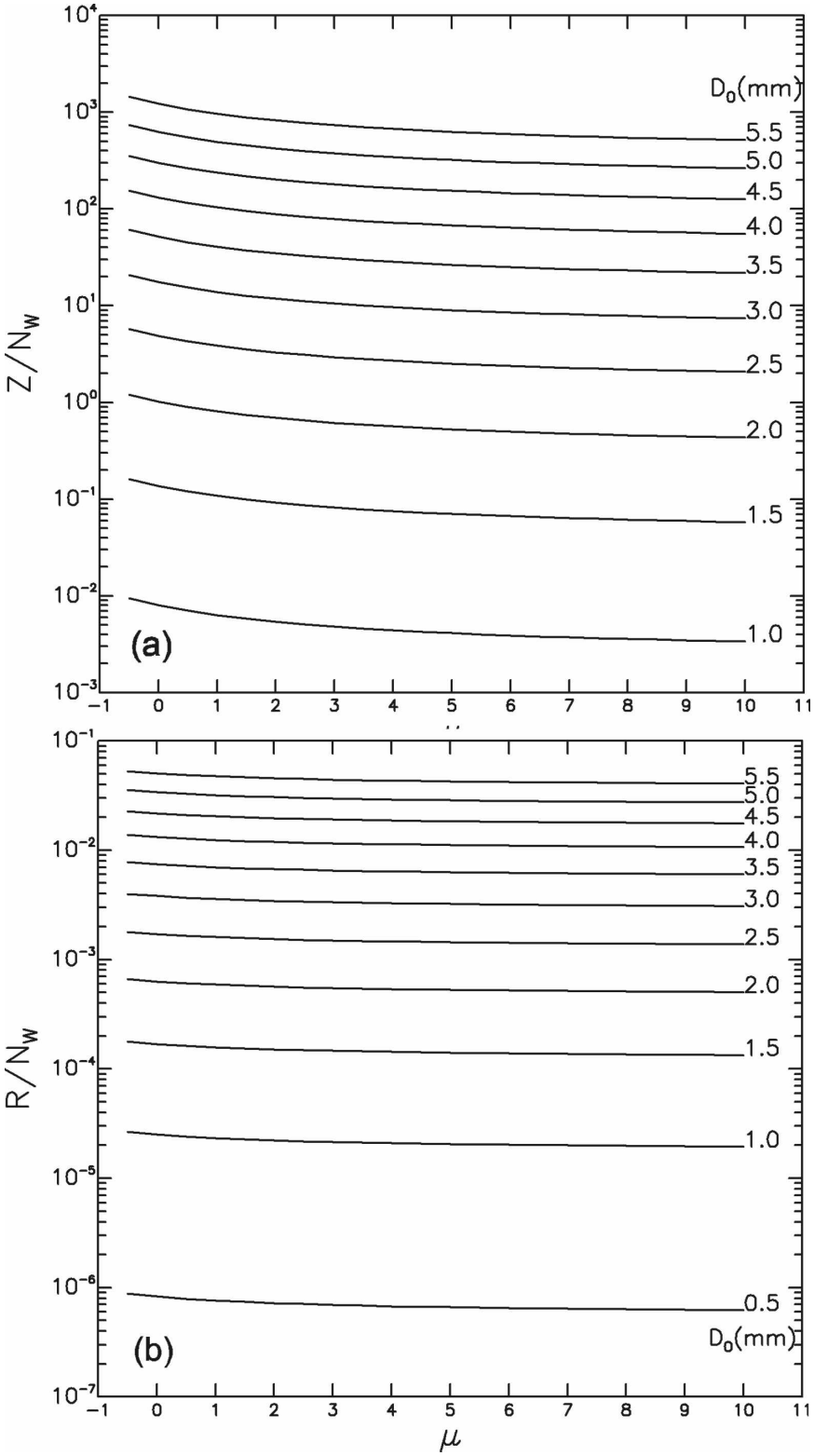

FIG. A1. The (a) Z/N_W and (b) R/N_W vs μ for values of $1 \leq D_0 \leq 5$ mm.

APPENDIX

Derivation of the Ratio R/Z as a Function of Z_{DR}

Using the Atlas et al. (1973) approximation to the drop fall speed, $v(D) = 9.65 - 10.3 \exp(-6D)$ (where D is in centimeters), the gamma DSD [Eq.(1)], and the relationship $\Lambda D_0 = 3.67 + \mu$, it may be shown from the definitions of the rainfall rate R (mm h^{-1}) and reflectivity factor Z (mm^6 m^{-3}) that

$$\frac{R}{Z} = \frac{0.6\pi\Gamma(4+\mu)(3.67+\mu)^3}{10^6\Gamma(7+\mu)D_0^3} \times \left[9.65 - 10.3\left(1 + \frac{6D_0}{3.67+\mu}\right)^{-(4+\mu)}\right]. \quad \text{(A1)}$$

The inverse of this relation can be written in the form $Z/R = F(\mu, D_0)D_0^3$ so that, for a given value of μ, when D_0 is constant, as in the convective parts of the storms considered here, then $Z \propto R$; that is, $Z = AR$, where A is a function of μ and D_0. A plot of A as a function of D_0 was shown in Fig. 4 for several values of μ. Because this work assumes that $D_0 = 0.295Z_{DR}^{2.06}$, Eq. (A1) is a relation between Z_{DR} and R/Z. This relation is depicted in the plot of Z_{DR} versus R/Z shown in Fig. 3 for values of $\mu = -1$, 0, 1, 5, and 12. In addition, the isopleths of D_0 and N_W shown in the advanced rain parameter diagram in Fig. 7 were constructed using Eq. (A1) and a value of $\mu = 5$. These isopleths are not strongly dependent on the value of μ. This is illustrated in Figs. A1a,b where Z/N_W and R/N_W, respectively, are plotted versus μ for several values of D_0. It is seen that, over the range of $-1 \leq \mu \leq 10$, R/N_W varies by only about 1 dB whereas Z/N_W varies by about 3 dB. These figures can be used to adjust values found from Fig. 6 for values of μ different from 5.

REFERENCES

Andreae, M. O., D. Rosenfeld, P. Artaxo, A. A. Costa, G. P. Frank, K. M. Longo, and M. A. F. Silva-Dias, 2004: Smoking rain clouds over the Amazon. *Science,* **303,** 1337–1342.

Atlas, D., and C. W. Ulbrich, 2000: An observationally based conceptual model of warm oceanic convective rain in the tropics. *J. Appl. Meteor.,* **39,** 2165–2181.

——, and ——, 2006: Drop size spectra and integral remote sensing parameters in the transition from convective to stratiform rain. *Geophys. Res. Lett.,* **33,** L16803, doi:10.1029/2006GL026824.

——, R. C. Srivastava, and R. S. Sekhon, 1973: Doppler radar characteristics at vertical incidence. *Rev. Geophys. Space Phys.,* **11,** 1–35.

——, C. W. Ulbrich, F. D. Marks, E. Amitai, and C. R. Williams, 1999: Systematic variation of drop size and radar-rainfall relations. *J. Geophys. Res.,* **104,** 6155–6169.

Battan, L. J., 1973: *Radar Observation of the Atmosphere.* University of Chicago Press, 324 pp.

Bringi, V. N., and V. Chandrasekar, 2001: *Polarimetric Doppler Weather Radar: Principles and Applications*. Cambridge University Press, 636 pp.

——, ——, J. Hubbert, E. Gorgucci, W. L. Randeu, and M. Schoenhuber, 2003: Raindrop size distribution in different climatic regimes from disdrometer and dual-polarized radar analysis. *J. Atmos. Sci.,* **60,** 354–365.

Chang, W.-Y., and T. C. Chen Wang, 2007: The characteristics of raindrop size distribution and drop shape relation in typhoon systems from 2D-video disdrometer and NCU C-band polarimetric radar. Preprints, *33rd Radar Meteorology Conf.,* Cairns, Australia, Amer. Meteor. Soc., 8A4. [Available online at http://ams.confex.com/ams/pdfpapers/122720.pdf.]

Fujiwara, M., 1965: Raindrop-size distribution from individual storms. *J. Atmos. Sci.,* **22,** 585–591.

Hu, R. C., and R. C. Srivastava, 1995: Evolution of raindrop size distributions by coalescence, breakup, and evaporation: Theory and observation. *J. Atmos. Sci.,* **52,** 1761–1783.

List, R., 1988: A linear radar reflectivity-rain rate relationship for steady tropical rain. *J. Atmos. Sci.,* **45,** 3564–3572.

Meneghini, R., and L. Liao, 2007: On the equivalence of dual-wavelength and dual-polarization equations for estimation of the raindrop size distribution. *J. Atmos. Oceanic Technol.,* **24,** 806–820.

Mueller, E. A., 1962: Raindrop size distributions in Miami, Florida. Research Rep. 9b, Illinois State Water Survey Meteorological Laboratory at the University of Illinois, 281 pp.

Pruppacher, H. R., and J. D. Klett, 1978: *Microphysics of Clouds and Precipitation.* D. Reidel, 714 pp.

Rosenfeld, D., 2000: Suppression of rain and snow by urban and industrial air pollution. *Science,* **287,** 1793–1796.

——, and C. W. Ulbrich, 2003: Cloud microphysical properties, processes, and rainfall estimation opportunities. *Radar and Atmospheric Science: A Collection of Essays in Honor of David Atlas, Meteor. Monogr.,* No. 52, Amer. Meteor. Soc., 237–258.

——, D. Atlas, and D. A. Short, 1990: The estimation of convective rainfall by area integrals. 2. The height-area rainfall threshold (HART) method. *J. Geophys. Res.,* **95,** 2161–2176.

——, M. Fromm, J. Trentman, G. Luderer, M. O. Andreae, and R. Servranckx, 2007: The Chisholm firestorm: Observed microstructure, precipitation and lightning activity of a pyro-Cb. *Atmos. Chem. Phys.,* **7,** 645–659.

Srivastava, R. C., 1967: A study of the effect of precipitation on cumulus dynamics. *J. Atmos. Sci.,* **24,** 36–45.

Testud, J., S. Ouray, R. A. Black, P. Amayenc, and X. Dou, 2001: The concept of "normalized" distribution to describe raindrop size spectra: A tool for cloud physics and cloud remote sensing. *J. Atmos. Sci.,* **40,** 1118–1140.

Tokay, A., D. A. Short, C. R. Williams, W. L. Ecklund, and K. S. Gage, 1999: Tropical rainfall associated with convective and stratiform clouds: Intercomparison of disdrometer and profiler measurements. *J. Appl. Meteor.,* **38,** 302–320.

Uijlenhoet, R., J. A. Smith, and M. Steiner, 2003: The microphysical structure of extreme precipitation as inferred from ground-based raindrop spectra. *J. Atmos. Sci.,* **60,** 1220–1238.

Ulbrich, C. W., and D. Atlas, 2007: Microphysics of raindrop size spectra: Tropical continental and maritime storms. *J. Appl. Meteor. Climatol.,* **46,** 1777–1791.